A REVIEW OF FINITE ELEMENT TECHNIQUES TO ANALYSE 3D PIEZOELECTRIC CRACK PROBLEMS

M. Kuna

Institute of Mechanics and Fluid Dynamics, Technische Universität Bergakademie Freiberg,
Lampadiusstraße 4, FREIBERG, D 09596, GERMANY

ABSTRACT

A review is given about present-day FEM-techniques to compute the coupled electromechanical boundary value problem of cracks in three-dimensional piezoelectric structures. The aim is to calculate the relevant fracture parameters very precisely and efficient, which requires to account for the singularity of the mechanical and electrical fields at crack tips in the numerical treatment. The following specialized techniques are presented in detail: i) Special singular crack tip elements, ii) Determination of intensity factors $K_I - K_{IV}$ from near tip fields, iii) Modified crack closure integral and iv) Computation of electromechanical J-integral. Special emphasis is devoted to different electric crack face boundary conditions. The accuracy, efficiency and applicability of these techniques are examined by various example problems and discussed with respect to their advantages and drawbacks for practical applications.

1   INTRODUCTION

Piezoelectric materials have widespread applications in modern technical areas such as mechatronics, micro system technology or smart structures, where they serve as sensors, actuators or transducers. For the assessment of strength and reliability of piezoelectric structures under combined electrical, mechanical and thermal loading, the existence of crack-like defects plays an important role. Fracture mechanics of piezoelectric materials has been established quite well in the last decade, see the review papers [1-2] including literature cited there. However, only a few exact solutions for three-dimensional (3D) crack problems are available, regarding circular or elliptic cracks in the infinite domain. Most of these solutions imply simplified electrical boundary conditions at the crack faces, assuming either an isolating or fully electrically permeable behavior, whereas real cracks are filled with dielectric or conducting media. Therefore, numerical methods as finite elements (FEM) are required to analyze realistic crack configurations and loading situations in technical components.

2   PIEZOELECTRIC FRACTURE MECHANICS

The constitutive equations (1) for a piezoelectric material relate the stress tensor σ_{ij} and the dielectric displacement vector D_i to the strain tensor ε_{ij} and the electric field E_i, where

$$\sigma_{ij} = c_{ijkl}\varepsilon_{kl} - e_{kij}E_k, \qquad\qquad D_i = e_{ijk}\varepsilon_{jk} + \kappa_{ij}E_j \qquad\qquad (1)$$

c_{ijkl}, e_{kij}, κ_{ij} are the elastic, piezoelectric and dielectric constants. At each point along the crack front the asymptotic electrical and mechanical fields [1-3] are controlled by the three known mechanical stress intensity factors (K_I, K_{II}, K_{III}) as well as the fourth "electric displacement intensity factor" K_{IV}, where $(r, \theta, x3) = (x1, x2, x3)$ is the crack tip coordinate system, see Fig. 1. The generalized tractions t on the ligament ahead of the crack $(\theta=0)$ have the singular form

$$\mathbf{t} = \left\{\sigma_{12}, \sigma_{22}, \sigma_{32}, D_2\right\}^T = \frac{1}{\sqrt{r}}\mathbf{f}\ \mathbf{K} \qquad\qquad \mathbf{K} = \left\{K_{II}, K_I, K_{III}, K_{IV}\right\}^T. \qquad (2)$$

The discontinuities of displacements u_i and electric potential φ across the crack faces behave as

$$\Delta\mathbf{u} = \mathbf{u}(r,\theta=\pi) - \mathbf{u}(r,\theta=-\pi) = \left\{\Delta u_1, \Delta u_2, \Delta u_3, \Delta\varphi\right\}^T = \sqrt{\frac{8r}{\pi}}\,\mathbf{Y}\,\mathbf{K}\,. \tag{3}$$

The energy release rate G is defined as the difference of total (electric enthalpy and mechanical potential) energy $\Delta\Pi_H$ in a structure, if the crack grows by an area ΔA. G_m and G_e denote the mechanical and electric terms of G. The relation to the intensity factors $\mathbf{K}$ is given by the generalized Irwin matrix $\mathbf{Y}$, which depends on the elastic, piezoelectric and dielectric material constants.

$$G = -\Delta\Pi_H/\Delta A = G_m + G_e = \frac{1}{2}\mathbf{K}^T\,\mathbf{Y}\,\mathbf{K} \tag{4}$$
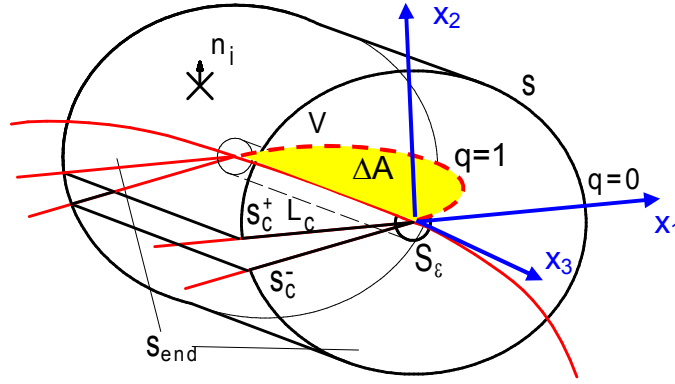
Fig. 1 Virtual crack extension ΔA along the crack front and J-integration domain

The electromechanical J_k^{em}-integral-vector is a generalization of Rice-Eshelby theory to cracks in 2D piezoelectric materials [1,2]. In the absence of body loads and inhomogeneities it becomes path-independent. Its x_1-component has the physical interpretation of energy release rate $J_1^{em} = G$. In the 3D case, a virtual crack extension l_k is considered along the crack front segment L_c with the area ΔA. Then, the released energy can be expressed by a surface integral (5) enclosing L_c.

$$-\Delta\Pi_H = \overline{J}^{em} = \int_S \left(H\,\delta_{kj} - \sigma_{ij}\,u_{i,k} + D_j\,E_k \right) l_k\,n_j\,dS\,, \quad \text{enthalpy density}\ H = \tfrac{1}{2}\left(\varepsilon_{ij}\,\sigma_{ij} - E_k\,D_k\right) \tag{5}$$

3 FINITE ELEMENT TECHNIQUES FOR 3D CRACK ANALYSIS

Finite element analysis of piezoelectric structures under combined mechanical and electric loadings is meanwhile available in several commercial codes. However, to deal with cracks requires some special techniques and know-how. Many of the numerical algorithms, developed for crack analyses in pure elastomechanics [4] and for 2D electromechanical cracks [5,6,7] can be generalized or adapted to the 3D coupled electromechanical crack problem.
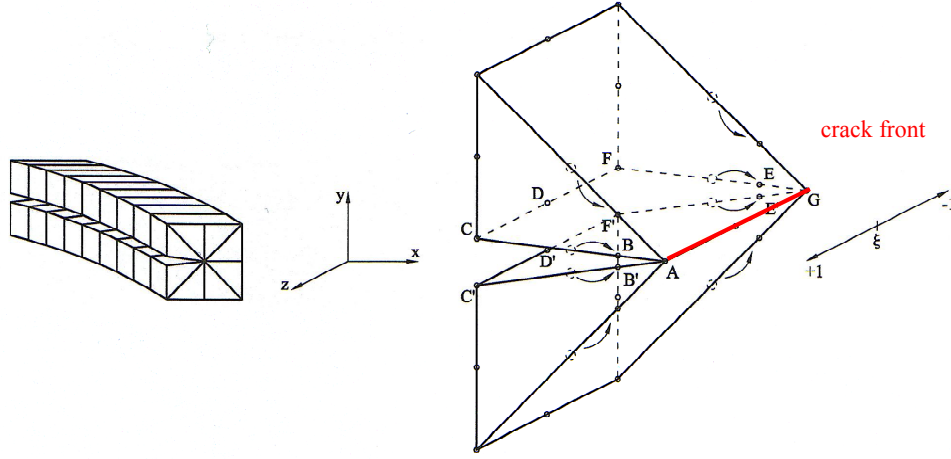
Fig. 2 Typical finite element mesh along crack front (left), 3D crack tip elements (right)

3.1   Singular electromechanical crack-tip elements (CTE)

In order to calculate accurate intensity factors, a proper representation of the crack tip singularity (2)(3) in the finite element approach is necessary. The simplest and most comfortable technique to create such special crack tip elements is a distortion of regular hexahedron (20 noded) or pentahedron (15 noded) elements with quadratic shape functions into so-called quarter-point elements.

It can be shown [4,7,8] that the shape functions are simply modified into a $r^{-1/2}$ behavior, if the mid-edge nodes are shifted into the ¼-position. Then, the crack front is discretized by groups of concentric pentahedron elements as illustrated in Fig. 2. The SIFs are obtained by comparing the analytical crack tip solution to the FEM results in the singular elements. A convenient formula for the vector **K** is deduced, if the discontinuities of the nodal displacements (3) across the crack faces $\Delta\mathbf{u}_B$ (indicated by letter B and B' etc.) are interpreted [9]   (6)

$$\mathbf{K}(\xi) = \sqrt{\frac{\pi}{8L}}\mathbf{Y}^{-1}\{2\Delta\mathbf{u}_B - \Delta\mathbf{u}_C + 2\Delta\mathbf{u}_E - \Delta\mathbf{u}_F + \Delta\mathbf{u}_D - \frac{\xi}{2}(4\Delta\mathbf{u}_B - \Delta\mathbf{u}_C - 4\Delta\mathbf{u}_E + \Delta\mathbf{u}_F) + \frac{\xi^2}{2}(\Delta\mathbf{u}_F + \Delta\mathbf{u}_C - 2\Delta\mathbf{u}_D)\}$$

The parameter ξ is the local element coordinate along the crack front. L denotes the length of the element edge between the nodes A and C or G and F.

3.2   Modified crack closure integral (MCCI)

Crack closure integrals [4,5,7] are well suited to compute the electromechanical energy release rate G for 3D crack problems [8,10], too. Assuming an arbitrary shaped finite advance of the crack front, G equals the electromechanical work per area ΔA during a virtual crack closure process.

$$G = \frac{1}{2\Delta A}\int_{\Delta A}\left[\mathbf{t}^*(r,\pi,x_3)\right]^T \Delta\mathbf{u}(r,-\pi,x_3)dA = G_m^I + G_m^{II} + G_m^{III} + G_e^{IV} \tag{7}$$

Here, the tractions $\mathbf{t}^* = \left\{\sigma_{12}^*,\sigma_{22}^*,\sigma_{32}^*,D_2^*\right\}^T$ correspond to the situation at the ligament before

crack growth $A = A_0$, whereas $\Delta \mathbf{u} = \left\{ \Delta u_1, \Delta u_2, \Delta u_3, \Delta \varphi \right\}^T$ denotes the values of crack opening displacements and electric potential difference after crack growth $A = A_0 + \Delta A$. The finite element realization of (7) leads to the MCCI technique. This means, G is approximated by multiplying the nodal forces F_{kj} and nodal charges ω_j in front of the crack tip with the corresponding nodal displacements Δu_{kj} and electric potential $\Delta \varphi_j$ behind the crack tip, see Fig. 3 and (8). The arc length along the crack front is denoted by w. The first index (k) indicates the coordinate direction and the second one (j) the corresponding pair of nodes. This procedure requires only one FEM calculation and can be utilized with regular [10] or singular [8] elements. There exist various schemes, how to weight the area parts ΔA_j corresponding to every node j. The best results were achieved by the choice given in (8), delivering G for the middle node.

$$G_m(w) = \frac{1}{2} \sum_{j=1}^{5} \frac{(F_{2j} \Delta u_{2j} + F_{1j} \Delta u_{1j} + F_{3j} \Delta u_{3j})}{\Delta A_j}, \qquad G_e(w) = \frac{1}{2} \sum_{j=1}^{5} \frac{(-\omega_j \Delta \varphi_j)}{\Delta A_j} \tag{8}$$

$$\Delta A_1 = \Delta A_2 = \Delta a_i (\Delta w_{i-1} + \Delta w_i), \qquad \Delta A_3 = \Delta a_i \Delta w_i, \qquad \Delta A_4 = \Delta A_5 = \Delta a_i (\Delta w_i + \Delta w_{i+1})$$
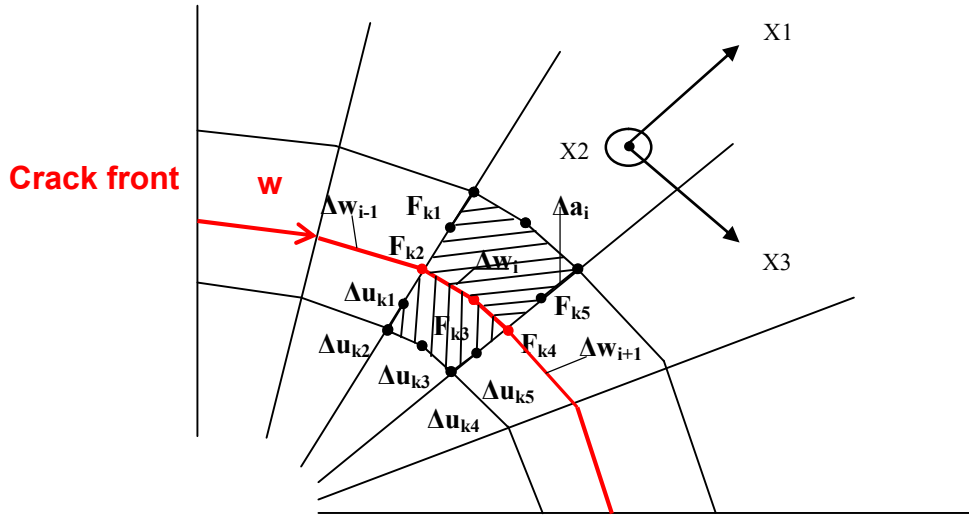
Fig. 3 Finite elements along three-dimensional crack front for MCCI

3.3   Electromechanical J-integral as equivalent domain integral (JEMD)

For the numerical computation of $\overline{J}^{em}$, it is advantageous to transform (5) into an equivalent domain integral over V. Therefore, a vectorial weighting function q_k is introduced, which equals the virtual crack extension l_k at the crack front L_c, but falls down to zero at the outer surface S and S_{end} . Finally, the local crack front value is found by $G(w) = \overline{J}^{em} / \Delta A$, see [11].

$$\bar{J}_k^{em} = -\int_V (H\,\delta_{kj} - \sigma_{ij}u_{i,k} + D_j\,E_k)\ q_{k,j}\,dV + \int_{S^+ + S^-} \left[H\,n_k - T_i u_{i,k} - \omega_S\,E_k\right]\ q_k\,dS \qquad (9)$$
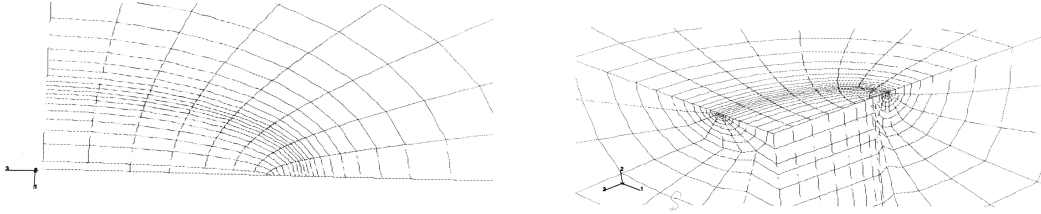
Fig. 4 Finite element mesh for an elliptical crack (1/4 model, 976 elements 4729 nodes)
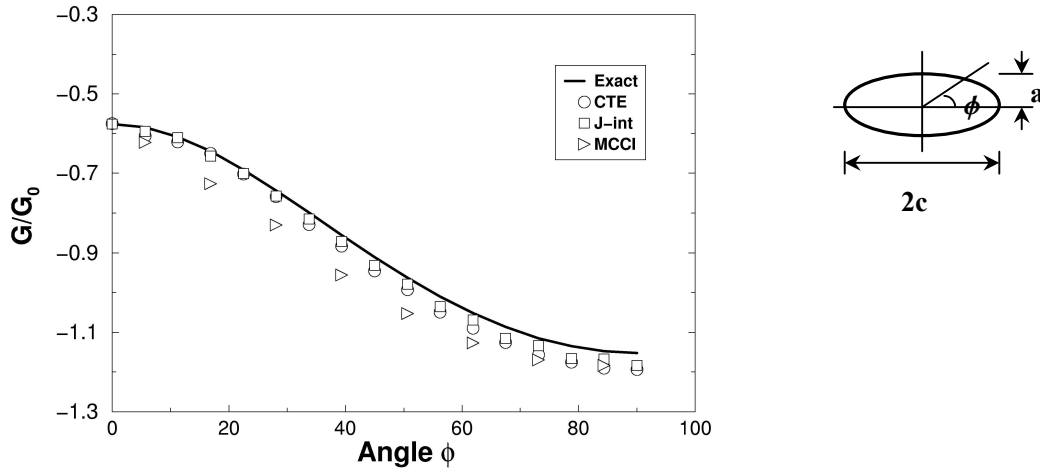
Fig. 5 *G* for embedded elliptical crack: Comparison of FEM-results with exact solution

4.   APPLICATION TO ELLIPTICAL CRACK PROBLEMS

As a verification example the embedded elliptical crack subjected to uniform normal traction σ_{22}^{∞} and electric surface charge D_2^{∞} has been investigated, see Fig. 5. The crack front position is described by the parametric angle ϕ of the ellipse with its semi-axes *c* and *a*. From the exact solutions [2,10] expressions of stress and electric field intensity factors were derived

$$K_I = g_I(a,c,\phi)\ \sigma_{22}^{\infty}\sqrt{\pi a}, \qquad K_{IV} = g_{IV}(a,c,\phi)\ D_2^{\infty}\sqrt{\pi a}, \qquad g_I = g_{IV} = \frac{(1 - k^2\cos^2\phi)^{1/4}}{E(k)} \qquad (10)$$

where $E(k)$ is the elliptical integral of the second kind with argument $k^2 = 1 - a^2/c^2$. The piezoelectric material PZT-5H is used with poling perpendicular to the crack. Fig. 4 shows a representative mesh and the details at the crack tip for an aspect ratio $c/a = 2$. The intensity factors K_I, K_{IV} computed by FEM with CTE-technique have an accuracy better than 1.5 % compared with (10). Also, the distributions of G achieved by the FEM-techniques of CTE, J-integral and MCCI agree well with the exact solution, as can be see in Fig. 5.

5 CONCLUSIONS

The developed FEM techniques provide a powerful tool to deal with 3D crack problems in piezoelectric materials. They are available for engineering applications, covering a wide range of more general crack configurations and loading situations. All three proposed finite element techniques for electromechanical crack analyses are verified by and applied to a variety of 3D crack problems [9-13]. All techniques can be easily implemented as post-processors for standard FEM codes, whereby the J-integrals requires the greatest effort and skill. The singular piezoelectric crack tip elements CTE yield most accurate predictions of electric and mechanical intensity factors compared to both other techniques. The implemented J-domain integral delivers the total energy release rate with highest precision and should be combined with CTE. Its path independence allows for inherent error control. A good accuracy for determining the energy release rate could be guaranteed by the modified crack closure integral technique with standard finite elements. Compared with the J-integral method, the MCCI-technique possesses the advantage that the energy release rate can be separated for the different mechanical opening modes (I, II, III) and the electric mode (IV). How limited crack permeability can be treated is shown in [12]. The generalization of FEM-techniques to 3D thermo piezoelectric crack problems is addressed in [13].

REFERENCES
[1] Qin, Q. H., Fracture mechanics of piezoelectric materials. WIT Press Southampton, 2001.
[2] Zhang, T.Y., Zhao, M.H., Tong, P., Advances in Appl. Mechanics. 38 (2002) 147-289.
[3] Wang, Z.K., Huang, S.H., Theor. Appl. Fracture Mech. 22 (1995) 229-237.
[4] M. H. Aliabadi, D.P. Rooke, Numerical Fracture Mechanics. Computational Mechanics Publications, Kluwer Academic Publisher, Southampton/Dordrecht/Boston/London (1991).
[5] Park, S., Sun, C.T., J. American Ceramics Soc. 78 (1995)1475-1480.
[6] Kumar, S., Singh, R.N., Acta Materialica 44 (1996) 173-200.
[7] Kuna, M., Computational Material Science 13 (1998) 67-80.
[8] Kemmer, G., Berechnung von elektromechanischen Intensitätsparametern bei Rissen in Piezokeramiken, Thesis TU Dresden, Fortschritt-Berichte, VDI Verlag Düsseldorf, 2000.
[9] Kuna, M., Ricoeur, A., In: Lynch, C.S., editor. Smart Structures and Materials, SPIE, Vol. 3992, 2000, p.185-196.
[10] Shang, F., Kuna, M., Abendroth, M., Eng. Fracture Mechanics 70 (2003)143-160.
[11] Abendroth, M., Groh, U., Kuna, M. and Ricoeur, A., Int. J. of Fracture 114 (2002), 359-378.
[12] K. Wippler, A. Ricoeur, M. Kuna., Eng. Fracture Mechanics (2004) to be published.
[13] Shang, F., Kuna, M., Scherzer, M., Int. J. Fracture 117 (2002), 113-128.